NANO LETTERS

LETTER

pubs.acs.org/NanoLett

Multicolored Vertical Silicon Nanowires

Kwanyong Seo,[†] Munib Wober,[‡] Paul Steinvurzel,[†] Ethan Schonbrun,[†] Yaping Dan,[†] Tal Ellenbogen,[†] and Kenneth B. Crozier*[,†]

[†]School of Engineering and Applied Sciences, Harvard University, Cambridge, Massachusetts 02138, United States

[‡]Zena Technologies, 174 Haverhill Road, Topsfield, Massachusetts 01983, United States

Supporting Information

ABSTRACT: We demonstrate that vertical silicon nanowires take on a surprising variety of colors covering the entire visible spectrum, in marked contrast to the gray color of bulk silicon. This effect is readily observable by bright-field microscopy, or even to the naked eye. The reflection spectra of the nanowires each show a dip whose position depends on the nanowire radii. We compare the experimental data to the results of finite difference time domain simulations to elucidate the physical mechanisms behind the phenomena we observe. The nanowires are fabricated as arrays, but the vivid colors arise not from scattering or diffractive effects of the array, but from the guided mode properties of the individual nanowires. Each nanowire can thus define its own color, allowing for complex spatial patterning. We anticipate that the color filter effect we demonstrate could be employed in nanoscale image sensor devices.

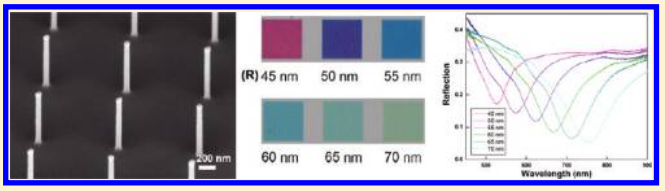

KEYWORDS: Vertical silicon nanowire, waveguiding, selective absorption, color filtering, photodetection

One-dimensional nanostructures often exhibit fascinating physical properties that are not observed in their bulk counterparts.[1−3] The optical properties of nanostructures are particularly sensitive to their physical dimensions. Consequently, nanostructures have yielded new methods for controlling light emission using quantum dots,[4] refractive index using metamaterials,[5] and scattering using localized surface plasmons.[6,7] Among recently investigated nanostructures, the silicon nanowire is one of the most important building blocks for nanoscale devices such as transistors,[8] photodetectors,[9] and solar cells.[10] Optical devices based on a silicon nanowire platform have been widely investigated of late, since they can be produced with existing complementary metal−oxide−semiconductor (CMOS) processing methods and so provide the most promising means to create high performance, low cost optical elements on the same size scale as integrated electronics. Here, we report a novel optical phenomenon of vertical silicon nanowires that is inherently due to nanoscale confinement effects. Bulk silicon appears gray in color, though it can be black if its reflectance is reduced by nanostructuring.[11,12] We show that vertical silicon nanowires take on a surprising variety of colors under bright-field illumination, which is a result of the radius-dependent wavelength selective waveguide mode excitation and subsequent light absorption by the individual vertical silicon nanowire. This single vertical silicon nanowire-based light control may provide opportunities to develop highly efficient nanowire based devices such as spectrally encoded optical data storage and image sensors.

We achieve precise control of the location, radius, and length of the nanowires via electron beam lithography (EBL) and inductively coupled-plasma reactive ion etching (ICP-RIE).[13−16] For experimental convenience, the nanowires are fabricated in arrays, although, the distinctive colors the nanowires exhibit are due to the properties of the individual wires, rather than of the array. The starting substrate is a single crystal silicon wafer. We fabricate an etch mask consisting of an array of aluminum disks using EBL and liftoff, then form the vertical nanowires by dry etching. Although some damage to the surface may result from etching, we anticipate that the nanowire core retains the electrical and optical properties of single crystal silicon.[13] To investigate surface roughness of the etched silicon nanowires, we performed atomic force microscopy (AFM) on a representative nanowire. The root-mean-square (rms) value of the surface height deviations is about 5 nm, which is about 2.5% of radius of the nanowire (Supporting Information, Figure S2). Figure 1 shows scanning electron microscope (SEM) images of a vertical silicon nanowire array. The square array shown in Figure 1a has a period of 1 μm, an overall extent of 100 μm × 100 μm, and therefore consists of 10 000 silicon nanowires. The radii of the nanowires are varied from 45 to 70 nm in 5 nm steps by different choices for the radius of the aluminum metal mask. The nanowires in Figure 1 have radii of 45 nm and are 1 μm long. The SEM images show excellent uniformity in the nanowire shape and size (Figure 1b−d). The images in Figure 1 are obtained prior to the removal of the aluminum disks. This is subsequently carried out by wet etching. The reflection measurements we present are obtained after this step.

Figure 2a shows bright-field optical microscope images of the nanowires, where each square consists of a 100 μm × 100 μm array of nanowires with a specific radius (R). The difference in color between the arrays is clearly apparent. Unlike what has been observed in horizontal nanowires by dark-field scattering,[17] the

Received: January 18, 2011
Revised: March 2, 2011
Published: March 17, 2011

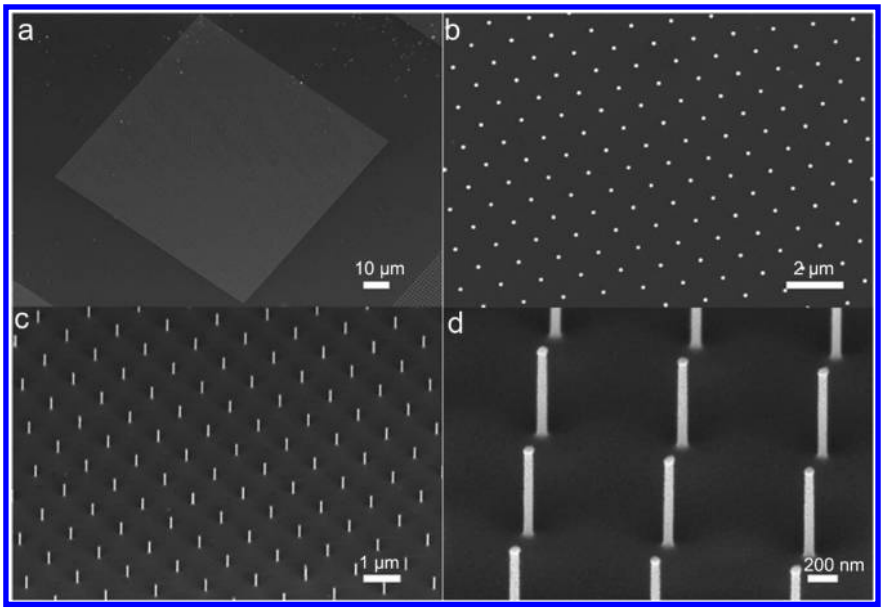

Figure 1. SEM images of vertical silicon nanowire array. (a) Vertical silicon nanowire square array. Overall extent of nanowire array is 100 μm by 100 μm. Nanowire pitch is 1 μm. Top view (b) and 30° tilted view (c) of nanowire array. (d) Magnified tilted view of nanowire array. The nanowires have radii of 45 nm and are 1 μm long.

color we observe in vertical silicon nanowires can be seen easily in a bright-field image and has only a weak dependence on the angle of illumination. As we will discuss later, this is a result of the radius-dependent wavelength selective coupling to the nanowire waveguide mode and underlying substrate. To quantify this phenomenon, reflection spectra were measured. As shown in Figure 2b, each reflection spectrum shows a dip, the position of which can be tuned over the full visible range by adjusting radius of the nanowire. Note that only one major spectral dip was observed in each spectrum, which is because only the fundamental mode is important in this process. Unlike the mechanisms by which nanoresonators or photonic crystals obtain their colors,[18,19] we rule out the role of diffractive or coupling effects in the origin of the color change by measuring arrays with the same nanowire radius but larger pitch (1.5 and 2 μm). We find the position of the spectral dip shifts less than 1% while the magnitude of extinction is reduced because fewer nanowires per unit area are illuminated. The same reflection measurements are performed with collimated illumination using a home-built setup, and the spectra are mostly unchanged relative to those obtained with focused illumination, although the each dip position shifts a few nanometers and the depth of the each dip is reduced, though by less than 10%. This indicates that features we measure are largely insensitive to the angle of illumination and can be understood by modeling the coupling dynamics for normally incident light. This was confirmed by angle-resolved reflection measurements with collimated illumination (Supporting Information, Figure S1). Figure 2b also shows that the depth of the dips increases monotonically with wavelength. The effect can be understood as follows. The transmittance and reflectance of plane waves at the interface between homogeneous media with different refractive indices are governed by the Fresnel equations.[20] These predict that the transmittance increases (and reflectance decreases) with decreasing index contrast between the media. Although the transmittance and reflectance of the guided mode at the silicon interface are not governed by the Fresnel equations, the basic trend that the transmittance increases (and reflectance decreases) with decreasing index contrast between the n_{eff} and n_{Si} still holds true. Here n_{eff} is the effective index of the waveguide mode of the nanowire, and n_{Si} is the index of the silicon substrate. The effective index of the waveguide mode n_{eff} at the maximum extinction point is always very near n_{air}, the refractive index of air. It is therefore to be expected that the coupling between the nanowire mode and substrate should increase, that is, that the transmittance should increase and the reflection decrease, as the substrate index decreases. Because the refractive index of silicon decreases with wavelength above bandgap,[21] the depth of the reflection dips are predicted to increase with wavelength by this reasoning. This is confirmed by the experimental data. Figure 2c shows simulated reflection spectra obtained using the finite difference time domain (FDTD) method. The simulated spectra are quantitatively in good agreement with the experimental results with respect to the spectral dip position as a function of nanowire radius. We also plot the dip position as a function of nanowire radius (Figure 2d) for both the experiments and simulations. Good agreement can be seen, with a linear dependence of dip position with nanowire radius. On the basis of the strong modulation depth of the reflectance, and the ability to modify the spectral dip position by appropriate choice of radius, the results suggest that silicon nanowire arrays could function as very efficient color filters over the full range of the visible region.

The wavelength selective reflection, transmission, and absorption of vertical silicon nanowire arrays originate from the strong wavelength dependence of the field distribution of the fundamental guided mode ($HE_{1,1}$ mode) supported by each nanowire. In Figure 3a, a schematic illustration is shown of the possible pathways for light normally incident on a nanowire. Light that does not interact with nanowire mode is reflected or transmitted at the bottom silicon/air interface according to the Fresnel equations. Light that does interact with the nanowire mode can be scattered at the top air/nanowire interface, absorbed along the nanowire length, and reflected or transmitted at the bottom

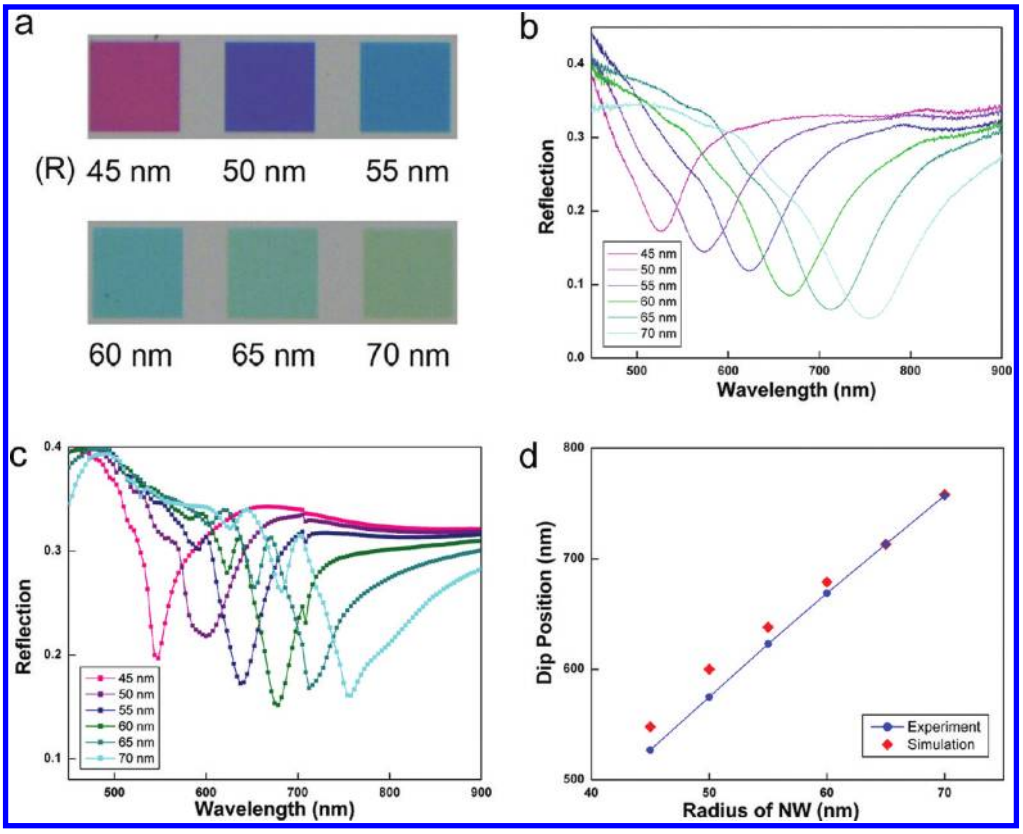

Figure 2. Reflection spectra of the vertical silicon nanowire arrays. (a) Bright-field optical microscope images of nanowire arrays. Nanowires with different radii appear distinctly different colors. (b) Measured reflection spectra of nanowire arrays. Spectra each show a spectral dip whose position depends on the nanowire radii. Spectral dip shifts to longer wavelengths as radius of the nanowire increases. (c) FDTD simulations of reflection spectra of nanowire arrays. The feature near 700 nm is due to the following. The nanowire array behaves as a grating with reflected orders in air appearing at $\lambda_{(n,m)} = (n_{air} \times a)/(n^2 + m^2)^{1/2}$, where n and m are integers. Since the refractive index of air (n_{air}) is unity and the pitch (a) is 1 μm, the (1,1) order appears at 707 nm. The appearance of new orders may lead to discontinuities, exacerbated by the challenge of numerically computing orders which, when they first appear, are propagating at 90° from normal. (d) Measured and simulated spectral dip positions as a function of nanowire radius.

silicon/nanowire interface. When considering the light that couples to the nanowire, only the $HE_{1,1}$ mode needs to be considered. Symmetry prevents efficient interaction with other guided modes in this system, and the nanowire dimensions are sufficiently small that we may generally ignore higher order $HE_{1,m}$ modes. We plot the major transverse component (E_y in this example) of the $HE_{1,1}$ mode at three representative wavelengths (Figure 3b−d) for a nanowire with a radius of 45 nm. At short wavelengths, the mode is tightly confined to the nanowire (Figure 3c). Unfocused light normally incident from free space does not efficiently excite the mode since the spatial overlap is extremely poor when it is so tightly confined. The other extreme occurs for longer wavelengths (Figure 3d) and exhibits a modal field that is mostly expelled from the silicon nanowire, instead comprising evanescent fields in the surrounding air. Although this mode can be efficiently excited from free space, it is delocalized from the nanowire with an effective index and absorption approaching that of air. We thus expect that at either end of the optical spectrum, the nanowire arrays should have reflection and transmission properties similar to a planar air/silicon interface under normal incidence. However, at some intermediate wavelength, corresponding to each dip of Figure 2b, the mode can both be excited from free space and non-negligibly interact with the nanowire. While the majority of the transverse field is in the air, some part of it is still localized in the nanowire (Figure 3b). This light can be either absorbed in the nanowire or efficiently coupled to the substrate. Furthermore, the large index contrast of the nanowire means the longitudinal field component (E_z) is non-negligible and has significant overlap with the nanowire. Since the modal absorption is proportional to the energy density, which includes E_z, it is therefore possible to obtain both efficient coupling and efficient absorption. The wavelength at which we get this trade-off between delocalization and confinement depends only on the nanowire radius, thus enabling a very simple yet versatile method to create spatially patterned color filters.

Figure 4a shows the effective index (n_{eff}) of the fundamental mode of the nanowire array (solved over a 1 μm unit cell with periodic boundaries) as a function of wavelength for nanowires with different radii. n_{eff} increases sharply and approaches n_{Si} for wavelengths shorter than the dip position shown in Figure 2. The dip position occurs where n_{eff} begins to asymptote to n_{air}. As we increase the nanowire radius, the dispersion curves, and the asymptotic point associated with the dip position, all shift to longer wavelengths as expected. From Figure 4b, it can be seen that for blue light (<500 nm), over 90% of the mode can be absorbed in a 1 μm length of the nanowire. Figure 4c shows FDTD simulation results corresponding to the absorption and reflection associated with 45 nm radius nanowires on a silicon substrate. The reflection dip (red circles in Figure 4c) is slightly red shifted in wavelength relative to the nanowire absorption

dx.doi.org/10.1021/nl200201b |*Nano Lett.* 2011, 11, 1851–1856

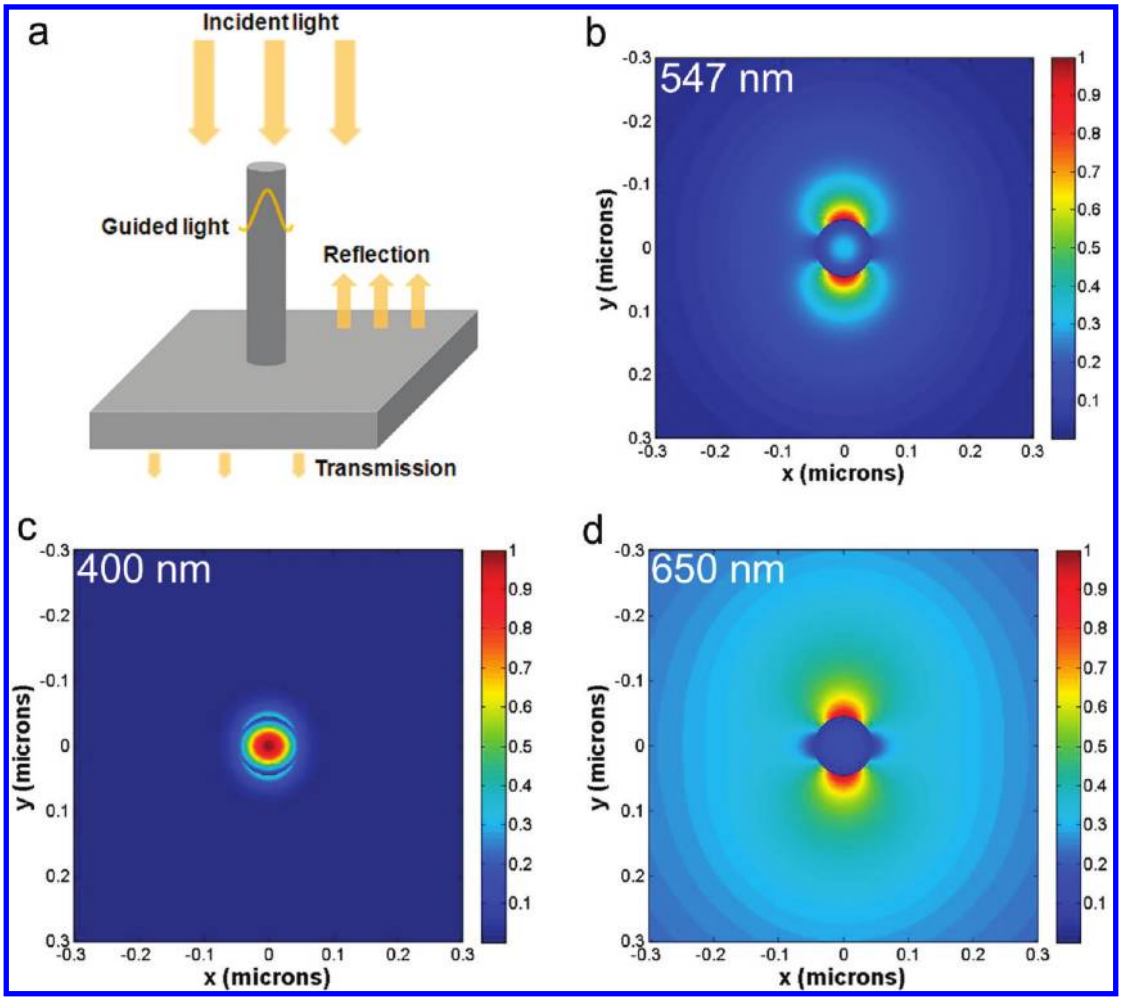

Figure 3. Wavelength selective coupling mechanism in vertical silicon nanowire arrays. (a) Schematic illustration of wavelength selective waveguiding system. (b−d) Major transverse electric field (E_y) distribution of fundamental mode of a 45 nm radius silicon nanowire for wavelengths of 547, 400, and 650 nm, respectively. There is a strong interaction between the nanowire and the incident field at 547 nm, but not at 400 or 650 nm. Fields are computed from the analytic formulas for the fundamental mode of a single nanowire in air. Numerical simulations for the dispersion of guided modes of a rectangular nanowire array with 1 μm pitch are almost identical to the single nanowire case below 570 nm; at 650 nm, there is nearest neighbor coupling to adjacent nanowires that affects the field distribution, but the mode is still expelled from the silicon core.

peak (blue circles in Figure 4c), which indicates that the long wavelength edge of the reflection dip arises more from coupling to the substrate. Nonetheless, this shows that the guided light is in fact absorbed in the nanowire core, and so the shape of the reflection spectrum and the amount of light absorbed in the nanowire can be controlled by altering the nanowire length. The light absorbed by the substrate (green circles in Figure 4c) can be enhanced or diminished by the nanowire relative to what one would get in the absence of the nanowires, depending on whether the nanowire absorbs or merely couples to the substrate. The fact that the filtering characteristics of the nanowire are related to absorption in different parts of the structure may be useful for applications in optoelectronic devices. For example, if one uses this structure as a photodetector and can compare the photocurrent extracted from the nanowire vs the substrate, one can make a multicolor pixel, or a coarse spectrometer.

The wavelength selective coupling to guided modes of vertical silicon nanowires suggests three application possibilities. First, colored surfaces are often required for decorative applications, and this work introduces an additional mechanism by which this may be achieved. Second, data storage could be performed through an array of cells, each of which contains multiple nanowires with different radii. Information could be encoded in the spectral dimension within each cell, through the presence or absence of nanowires with specific radii in a conceptually similar manner to that proposed using metallic nanoparticles observed by dark-field imaging[6] with the advantage that the readout can be done under bright-field illumination. Third, nanowire arrays could be used as color filters in digital image sensors, but with the important advantage that the nanowires would also perform photodetection. Each nanowire could be fabricated above a photodetector in the substrate, with part of the spectrum detected by the nanowire, and part by the substrate photodetector. In this way, color separations could be performed without the use of absorptive color filters, which are optically inefficient. To illustrate this possibility, we design and fabricate large-scale vertical silicon nanowire arrays as shown in Figure 5a (30° tilted SEM image). The nanowire radii vary from 35 to 75 nm and the pitch and length are 1 μm as before. Figure 5b shows a bright-field optical microscope image of the pattern that exhibits colors covering the full

dx.doi.org/10.1021/nl200201b |*Nano Lett.* 2011, 11, 1851–1856

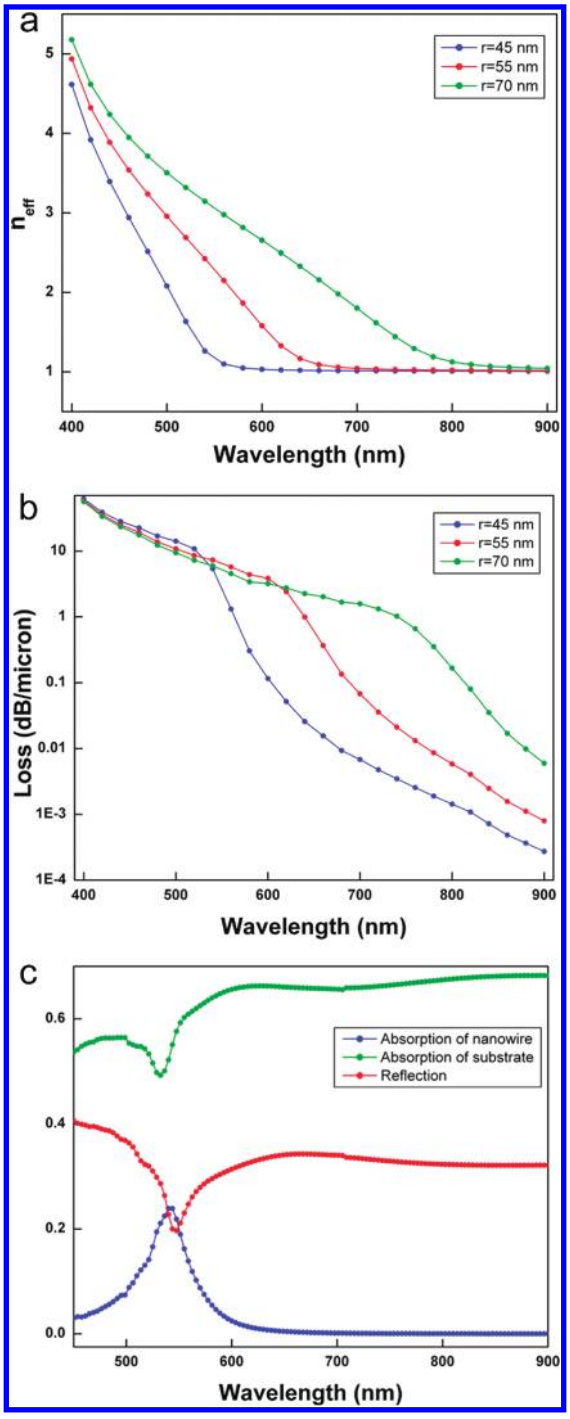

Figure 4. Wavelength selective coupling: simulation results. (a) n_{eff} as a function of wavelength of the fundamental mode of silicon nanowire arrays. (b) Loss in dB/micrometer as a function of wavelength of the fundamental mode of silicon nanowire arrays. Blue, red, and green circles are for radii of 45, 55, and 70 nm, respectively. (c) FDTD simulations of nanowire absorption, substrate absorption, and reflectance for arrays of silicon nanowires with radii of 45 nm. Nanowires are 1 μm long and are in a square array with a pitch of 1 μm.

visible spectrum. The color bars located both right top and bottom show a gradual color change resulting from the gradual variation of the nanowire radius. The magnified image of the selected area indicated by the white square in Figure 5b confirms

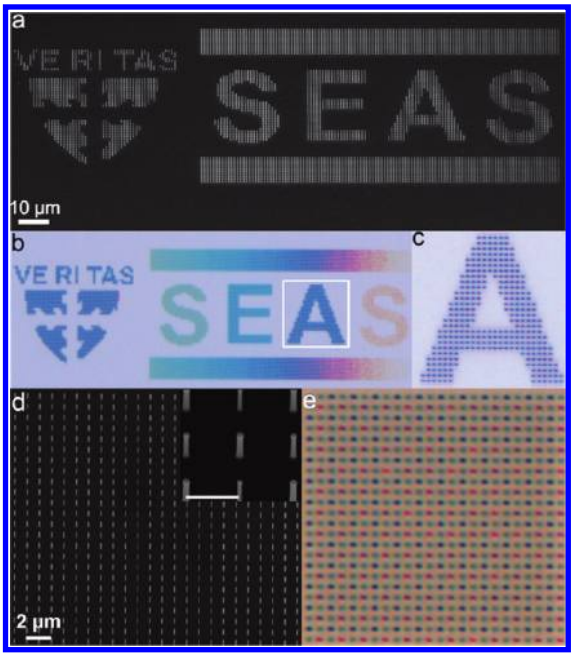

Figure 5. Patterned vertical silicon nanowire arrays. (a) A 30° tilted SEM image of vertical silicon nanowire array pattern. Radii of the nanowires vary from 35 to 75 nm and the length of the nanowire is ~1 μm. Letters S (left), E, A, and S (right) each comprise nanowires with radii of 70, 60, 50, and 40 nm, respectively. (b) Bright-field optical microscope image of pattern. Gradual color change is achieved by gradual change of nanowire radii. (c) Magnified image of the selected area indicated by the white square of panel b. Each blue spot is a single nanowire. (d) A 30° tilted SEM image of Bayer filter pattern. Pattern consists of vertical silicon nanowires with radii of 45, 50, and 65 nm representing red, blue, and green colors, respectively. Inset: magnified SEM image. Scale bar is 1 μm. (e) Bright-field optical microscope image of pattern. Each nanowire shows a color that can be controlled by appropriate choice of its radius.

that single nanowires can act as independent pixels showing color. We also fabricate a pattern of vertically standing silicon nanowires with three different radii of 45, 50, and 65 nm representing red, blue, and green, respectively. This is analogous to the Bayer filter employed in color image sensors. The bright-field image of the filter pattern clearly demonstrates that the color of the each nanowire can be controlled independently (Figure 5e). The results of Figure 5 provide further evidence that the color of nanowire originates not from diffractive or coupling effects of the array but from waveguiding effects.

In summary, we have demonstrated that vertical silicon nanowire arrays viewed under bright-field illumination can show various vivid colors over the full range of the visible spectrum in marked contrast to the gray color in bulk. The reflection spectra show a dip, the position of which red shifts with increasing nanowire radius, and this matches well with FDTD simulations. This surprising finding can be ascribed to the wavelength selective coupling to the guided nanowire mode. Thus, each nanowire can possess its own individual color independent of its neighbors. We anticipate that our technique could be advantageous for nanoscale optical applications such as image sensor devices.

■ ASSOCIATED CONTENT

Ⓢ Supporting Information. Detailed descriptions of methods, supplementary figures, and supplementary discussions. This

dx.doi.org/10.1021/nl200201b |*Nano Lett.* 2011, 11, 1851–1856

material is available free of charge via the Internet at http://pubs.acs.org.

AUTHOR INFORMATION

Corresponding Author

*Address: MD147, 33 Oxford Street, Cambridge, MA 02138. Tel: 617-496-1441. Fax: 617-495-2489. E-mail: kcrozier@seas.harvard.edu.

ACKNOWLEDGMENT

This work was supported by Zena Technologies. P.S. and T.E. acknowledge support from the Center for Excitonics, an Energy Frontier Research Center funded by the U.S. Department of Energy, Office of Science and Office of Basic Energy Sciences under Award Number DE-SC0001088. Fabrication work was carried out in the Harvard Center for Nanoscale Systems (CNS). We thank Dr. Boris Kuhlmey for many useful discussions.

REFERENCES

(1) Hu, J.; Odom, T. W.; Lieber, C. M. *Acc. Chem. Res.* **1999**, *32*, 435–445.

(2) Xia, Y.; Yang, P.; Sun, Y.; Wu, Y.; Mayers, B.; Gates, B.; Yin, Y.; Kim, F.; Yan, H. *Adv. Mater.* **2003**, *15*, 353–389.

(3) Yang, P.; Yan, R.; Fardy, M. *Nano Lett.* **2010**, *10*, 1529–1536.

(4) Murray, C. B.; Kagan, C. R.; Bawendi, M. G. *Annu. Rev. Mater. Sci.* **2000**, *30*, 545–610.

(5) Pendry, J. B.; Schurig, D.; Smith, D. R. *Science* **2006**, *312* 1780–1782.

(6) Ditlbacher, H.; Krenn, J. R.; Lamprecht, B.; Leitner, A.; Aussenegg, F. R. *Opt. Lett.* **2000**, *25*, 563–565.

(7) Bohren, C.; Huffmann, D. *Absorption and scattering of light by small particles*; Wiley: New York, 1983.

(8) Patolsky, F.; Timko, B. P.; Yu, G.; Fang, Y.; Greytak, A. B.; Zheng, G.; Lieber, C. M. *Science* **2006**, *25*, 1100–1104.

(9) Yang, C.; Barrelet, C. J.; Capasso, F.; Lieber, C. M. *Nano Lett.* **2006**, *6*, 2929–1934.

(10) Tian, B.; Zheng, X.; Kempa, T. J.; Fang, Y.; Yu, N.; Yu, G.; Huang, J.; Lieber, C. M. *Nature* **2007**, *449*, 885–889.

(11) Shen, M.; Carey, J. E.; Crouch, C. H.; Kandyla, M.; Stone, H. A.; Mazur, E. *Nano Lett.* **2008**, *8*, 2087–2091.

(12) Zhu, J.; Yu, Z.; Burkhard, G. F.; Hsu, C. -M.; Connor, S. T.; Xu, Y.; Wang, Q.; McGehee, M.; Fan, S.; Cui, Y. *Nano Lett.* **2009**, *9*, 279–282.

(13) Huang, Z.; Fang, H.; Zhu, J. *Adv. Mater.* **2007**, *19*, 744–748.

(14) Zhang, A.; You, S.; Soci, C.; Liu, Y.; Wang, D.; Lo, Y.-H. *Appl. Phys. Lett.* **2008**, *93*, No. 121110.

(15) Garnett, E.; Yang, P. *Nano Lett.* **2010**, *10*, 1082–1087.

(16) Pevzner, A.; Engel, Y.; Elnathan, R.; Ducobni, T.; Ben-Ishai, M.; Reddy, K.; Shpaisman, N.; Tsukernik, A.; Oksman, M.; Patolsky, F. *Nano Lett.* **2010**, *10*, 1202–1208.

(17) Cao, L.; Fan, P.; Barnard, E. S.; Brown, A. M.; Brongersma, M. L. *Nano Lett.* **2010**, *10*, 2649–2654.

(18) Kim, H.; Ge., J.; Kim, J.; Choi, S. −e.; Lee, H.; Lee, H.; Park, W.; Yin, Y.; Kwon, S. *Nat. Photonics* **2009**, *3*, 534–540.

(19) Xu, T.; Wu, Y. -K.; Luo, X.; Guo, L. J. *Nat. Commun.* **2010**, *1*, 59.

(20) Saleh, B. E. A.; Teich, M. C. *Fundamentals of Photonics*; Wiley: New York, 1991.

(21) *Handbook of Optical Constants*; Palik, E. D., Ed.; Academic Press: Orlando, FL, 1985.

NOTE ADDED AFTER ASAP PUBLICATION

The values of the radii were changed in the caption of Figure 5 and in the second to the last paragraph of the manuscript in the version of this paper published March 17, 2011. The correct version published March 31, 2011.